Lattice location and perturbed angular correlation studies of implanted Ag in $SrTiO_3$

A. C. Marques* [1,3], U. Wahl[1,2], J. G. Correia[1,2,3], E. Rita[1,2], J. C. Soares[1]

[(1)]*Centro de Física Nuclear da Universidade de Lisboa, Portugal*
[(2)]*Instituto Tecnológico e Nuclear, Sacavém, Portugal*
[(3)]*CERN, Geneva, Switzerland*

Abstract
Lattice site location and local environment characterization of implanted ^{111}Ag in $SrTiO_3$ by means of the emission channeling (EC) and γ-γ perturbed angular correlation (PAC) techniques are reported. The angular distribution of β^--particles emitted from the ^{111}Ag decay was monitored with a position-sensitive detector as a function of annealing temperature up to 900ºC. In the as-implanted state Ag occupies several lattice sites in $SrTiO_3$. Upon annealing, near-Sr and near-Ti occupancies increased to 58% and 28%, while an octahedral interstitial fraction vanished. Ag on near-Sr and near-Ti sites are still displaced by ~0.2-0.5 Å from ideal cubic positions. Subsequent PAC measurements confirmed that ~20% of ^{111}Ag atoms are in specific sites of non-cubic environment, characterized by a unique electrical-field-gradient (EFG), while ~80% were subject to a wide EFG distribution.

PACS codes: 61.72.Ww, 61.85.+p
Keywords: lattice location, ion implantation, $SrTiO_3$:Ag, emission channeling

Introduction

$SrTiO_3$ is a perovskite-type oxide with a band gap of 3.2 eV, with a great potential for microelectronic applications due to its extremely high bulk dielectric constant. Recently, $SrTiO_3$ has been epitaxially grown on Si (100) opening the route to devices based on metal-oxide heterostructures such as field effect transistors with $SrTiO_3$ gate dielectric for new high-density random access memories [1, 2] (FETs). This opens up the possibility of FETs with functional gate oxides with ferroelectric, superconducting, or magnetoresistive properties [1]. $SrTiO_3$ also has interesting and complex electrical and optical properties that can be modified by the incorporation of dopants, e.g., it acts as a n-type semiconductor upon substituting Nb^{5+} or Sb^{5+} for Ti^{4+} and as p-type upon substituting Sc^{3+} or La^{3+} for Ti^{4+} [3, 4]. The doping with rare-earth elements during growth has been reported [5] to induce changes in its optical and electric properties. $SrTiO_3$ rendered amorphous by ion implantation to recrystallize at low temperatures, already at 400°C [6], which means that implantation could represent an attractive approach for doping. However, little is known on the lattice site location of implanted impurities and remaining point defects in their neighborhood. For instance Ag, as a *4d* transition metal of group *Ib*, could also act as an acceptor in $SrTiO_3$ if incorporated on substitutional Sr sites. Recently, lattice site location of ^{167m}Er [7] implanted in $SrTiO_3$ was studied by means of emission channeling (EC). This work presents and discusses results of lattice site location of implanted Ag^+ ions in $SrTiO_3$, as a function of annealing temperature, which are complemented with firsts studies of the Ag microscopic surroundings, by means of the γ-γ perturbed angular correlation (PAC) technique.

Experimental Details

A commercially available $SrTiO_3$ single crystal sample [8], grown by the flame fused Verneuil method, cut and polished on a <100> surface, was implanted at room temperature with 60 keV $^{111}Ag^+$ ions up to a dose of $1x10^{13}$ atoms/cm^2 at the CERN-ISOLDE facility. A well-defined depth profile was made by tilting the beam 7º angle off the crystal surface normal, to minimize the fraction of ions channelled during implantation.

^{111}Ag decays with 7.45d half–life, by β^- particle emission, to the stable ^{111}Cd isotope. On their way out of the crystal, the β^- particles are guided by the mean crystal potentials, which are defined by the principal axis and planes of the lattice. These will redistribute the electron intensity, generating anisotropic yield maps that uniquely depend from the lattice site of the emitter atom, which are measured with a position sensitive detector described in Ref. [9]. Within an energy window set in the ^{111}Ag β^- continuum spectrum, from 40 keV up to the β^- endpoint energy of 1.03 MeV, the angular distributions were measured at room temperature, around the <111>, <100>, <110> and <211> axial directions, in the as-implanted state and after 10 min isochronical *in* situ vacuum annealing at 300°C, 600°C, 800°C and 900°C. The subsequent quantitative evaluation of the Ag^+ lattice site locations in the $SrTiO_3$ was achieved by comparing the observed angular distributions with simulated patterns for Ag on substitutional Sr, Ti and O and a variety of interstitial sites located along <100>, <110> or <111> in between the atomic positions. For instance, the <100>, <110> and <211> directions allow discriminating between Sr and Ti sites while the <110> direction consists of mixed rows of Sr and Ti atoms. The ^{111}Ag theoretical EC patterns were calculated by means of the "many beam" formalism for electron diffraction in single crystals [10]. To describe the $SrTiO_3$ perovskite structure a lattice constant of 3.905 Å and isotropic root mean square (rms) displacements of $u_1(Sr)=0.0773$ Å, $u_1(Ti)=0.0606$ Å and $u_1(O)=0.0848$ Å at 300

K were considered [11]. In the simulations, the angular range of 0º-3º around each of the investigated crystal directions was considered in small steps of $\Delta x = \Delta y = 0.05^{\circ}$.

The PAC technique was performed on the 900ºC annealed EC sample to probe the interaction of ^{111}Ag/^{111}Cd with remaining defects. The 96.7-245.4 keV gamma cascade on ^{111}Cd, obtained from the ^{111}Ag decay, was analyzed in a four- BaF_2 detector setup, arranged in a plane with 90º between adjacent detectors. Delayed coincidence spectra N(θ, t) were recorded for the detector angles of θ=90º and θ= 180º. From these spectra the experimental time differential anisotropy $R(t) = 2\left[N(180^{\circ},t) - N(90^{\circ},t)\right] / \left[N(180^{\circ},t) + 2 \times N(90^{\circ},t)\right]$ was calculated. Details of the calculation of the experimental R(t) function and of the theoretical fit can be found in ref. [12]. From these spectra, the electric field gradients (EFGs) produced by the surrounding charge distribution of ^{111}Cd (^{111}Ag) are analyzed. Due to symmetry reasons, the EFG tensor vanishes if the charge distribution around a particular site is of cubic symmetry. Since the EFG drops with $1/r^3$, r being the distance from the generating charges, mainly deviations from cubic symmetry in the first- and the second- nearest- neighbors, surrounding the probe nuclei lead to measurable effects.

Results and discussion

Figs. 1 (a)-(d) show the normalized β^- emission yields measured in the vicinity of the <111>, <100>, <110> and <211> directions following room temperature implantation of ^{111}Ag and annealing for 10 min at 900ºC. From the fact that channeling effects are observed along all major crystalline axes and planes it is obvious that the majority of Ag atoms must occupy substitutional sites or sites which are close to the substitutional positions. However, especially the <211> effects indicate that only a smaller fraction of Ag is occupying Ti sites, because Ti sites lead to a characteristic double peak structure along this direction, which is not observed in the experiment [7]. The best fits of the simulated patterns to the experimental ones are shown in Fig.1(e)-(h) and they result from considering three fractions for the Ag atoms, namely, substitutional Ag on Sr and Ti sites, and random sites. The best fits at the referred annealing temperature revealed that 59% of Ag atoms occupied near-Sr sites with rms displacements of $u_1(Ag_{Sr})$=0.215 Å and 24% near Ti sites with $u_1(Ag_{Ti})$=0.2 Å, and the remainder random sites. The rms displacements from Sr and Ti substitutional sites are similar to each other but significantly larger than the thermal vibration amplitude of the Sr atoms of u_1(Sr)=0.0773 Å and of the Ti atoms of u_1(Ti)=0.0606 Å. These high displacement values might be due to Ag interaction with remaining point defects, as will be later discussed.

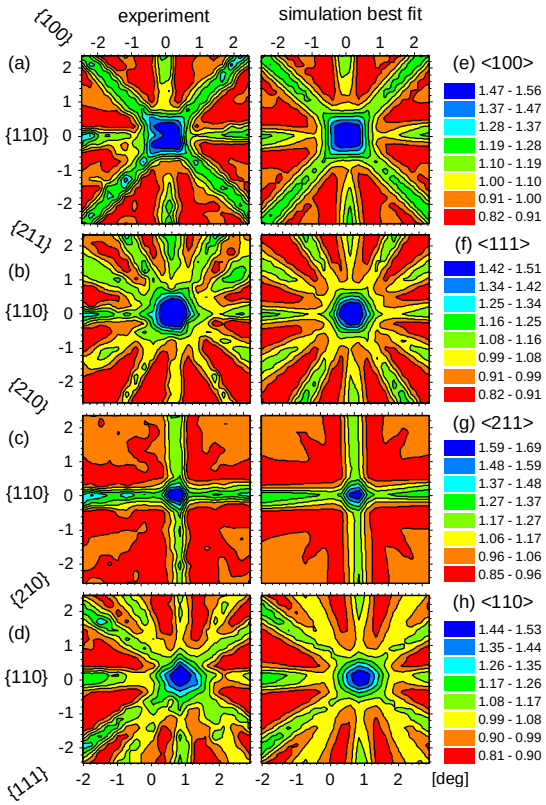

Figure 1: Angular distributions of β^- particles emitted from ^{111}Ag in $SrTiO^3$ around the <111> (a), <100> (b), <110> (c) and <211> (d) directions following room temperature implantation of ^{111}Ag and annealing for 10 min at 900ºC. The best fits of the simulated patterns to the experimental ones are shown in Fig.1(e)-(h).

Figure 2 shows the results of the complete annealing sequence. Besides Ag on near-Sr, near-Ti and random sites in the as implanted state an additional fraction of 11% of Ag on octahedral interstitial sites was found. This was revealed by the fact that fit quality improved for all angular distributions if octahedral interstitial sites were included in the fit. The octahedral interstitial sites are located midway between two Sr atoms, i.e. 1.953 Å from a Sr site along <100> directions but also midway between two Ti atoms, i. e. $\sqrt{2} \times 1.953$ Å from a Ti site along <110>. Upon annealing at 300°C the interstitial fraction of Ag completely disappeared, with the Ag fraction near Sr sites starting to grow in. Both substitutional Ti and Sr fractions increased further following annealing up to 800°C. Following annealing at 900°C some of the Ag atoms seem to have been promoted from near-Sr sites to near Ti sites.

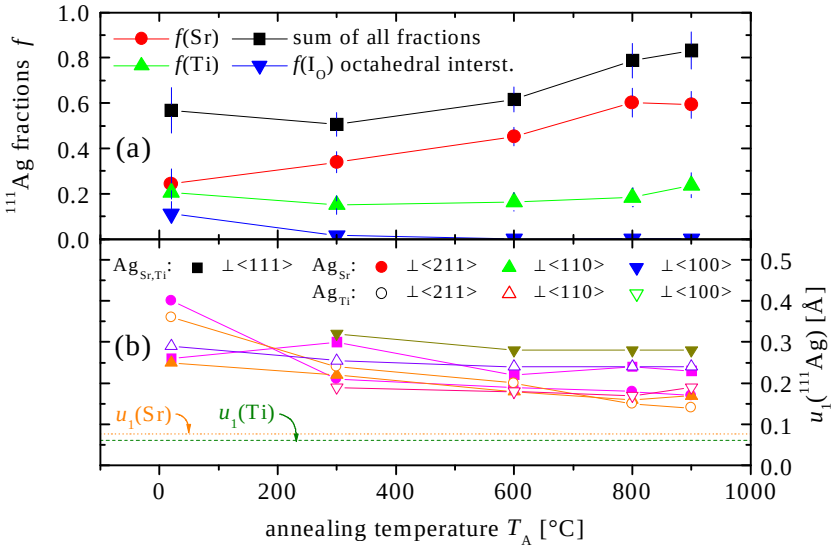

Figure 2: Substitutional fractions of Ag occupying Sr, Ti and octahedral interstitial sites and their rms displacements perpendicular to <111>, <100>, <110> and <211> axial directions as a function of annealing temperature in vacuum for 10 min. The dotted and dashed lines represent the room temperature Sr and Ti vibration amplitudes, respectively.

Figure 3 (a) shows the R(t) PAC experimental function and (b) its Fourier transform measured from the same EC sample, after the vacuum annealing at 900°C. The R(t) function shows a strong damping that reveals most of the ^{111}Cd atoms to be still interacting with defect distributions, with non-cubic local symmetry. Since the PAC measurement is done on ^{111}Cd, after the ^{111}Ag decay, it should be discussed if the Cd is on the same site as its precursor Ag atom. In fact, during decay the β^- particles with end-point energy of 1.03 MeV import to the Cd atoms a recoil energy less than 5 eV, which is not enough to create Frenkel pairs or move Cd atoms away from the Ag sites. Additionally, ongoing PAC experiments with ^{111m}Cd/^{111}Cd directly implanted in $SrTiO_3$ reveal Cd atoms to occupy unique lattice sites. Therefore the frequency distributions observed in the current work must depend on ^{111}Ag interaction with remaining defects. The ^{11m}Cd/^{111}Cd PAC experiments also showed that the local environment of Cd atoms only recovers to almost perfect cubic symmetry for annealing at 1000°C, indicating that point defects do not completely recover at lower annealing temperature. In the case of ^{111}Ag 20% of the Ag/Cd atoms interact with a well defined EFG_1, characterized by ω_0 = 81.8 ± 1.0 MRad/s and a small asymmetry parameter, η = 0.13 ± 0.02. The comparison of PAC and EC fractions therefore suggests that 20% of Ag near Ti sites corresponds to the fraction of Ag experiencing EFG_1, revealing the presence of a specific defect in the Ag_{Ti} neighborhood. The fact that the remaining 80% of Cd atoms interact with a broad EFG distribution hints that both the Ag atoms on near Sr sites as well as those on *random* sites are considerably influenced by nearby point defects. However, in contrast to Ag_{Ti}, there is no evidence for a specific configuration that would lead to a well defined EFG, i.e. a new characteristic frequency set in the PAC R(t) spectrum.

Conclusions

Following the ^{111}Ag low dose room temperature implantation of a $SrTiO_3$ crystal, the Ag atoms mainly occupy near-substitutional Sr and Ti sites with high root mean square displacements. With the exception of the as-implanted state, no evidence was found of Ag at other regular sites. The high displacement values seem to be due to Ag interaction with point defects, which remain in the lattice even upon annealing to 900°C. Therefore, our ^{111}Ag PAC experiments suggest that higher temperatures might be needed to allow for full recovery of implantation point defects in the Ag environment, which is also probably required for the electric activation of Ag. In fact, ongoing PAC experiments with ^{111m}Cd in $SrTiO_3$ suggest that radiation damage associated with the implantation process of the crystal is only fully recovered at 1000°C, which is well above the recrystallization temperature of amorphous $SrTiO_3$ as reported in ref. [6].

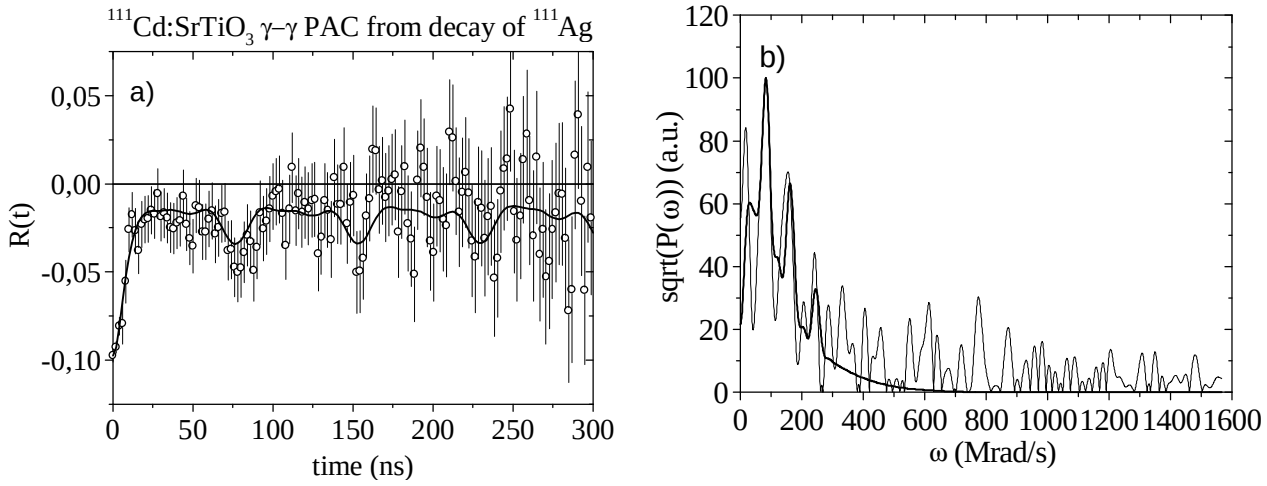

Figure 3: PAC anisotropy ratio R(t) (a) and its Fourier transform (b) obtained on the ^{111}Ag/^{111}Cd:SrTiO$_3$ system, with the <100> axis in detector plane at 45º with detectors. The thicker solid line on the R(t) and Fourier spectra represents the theoretical fit.

Acknowledgments

This work was funded by FCT, Portugal under project POCTi-FNU-49503-2002. A. C. Marques, E. Rita and U. Wahl acknowledge their PhD and post-doc fellowships supported by FCT. Special thanks are due to Roberto Amendolia for financial support of this work by his CERN group.

References

1] K. Eisenbeiser, J.M. Finder, Z. Yu, J. Ramdani, J.A. Curless, J.A. Curless, J.A. Hallmark, R. Droopad, W.J. Ooms, L. Salem, S. Bradshaw, and C.D. Overgaard, Appl. Phys. Lett. 76 (2000) 1324.

[2] C. J. Först, C. R. Ashman, K. Schwarz, and P. Blöchl, Nature 427 (2003) 53

[3] T. Higuchi, T. Tsukamoto, K. Kobayashi, S. Yamaguchi, Y. Ishiwata, N. Sata, K. Hiramoto, M. Ishigame, and S. Shin, Phys. Rev. B 65 (2001) 033201.

[4] H.H. Wang, F. Chen, S.Y. Dai, T. Zhao, H.B. Lu, D.F. Cui, Y.L. Zhou, Z.H. Chen, and G.Z. Yang, Appl. Phys. Lett. 78 (2001) 1676.

[5] L.J. Knott, N.J.Cockroft, J.C. Wright, Phys. Rev. B 51 (1995) 5649, and references therein.

[6] C.W. White, L.A. Boatner, P.S. Sklad, C.J. Mc Hargue, J. Rankin, G.C. Farlow, and M.J. Aziz, Nucl. Instr. Meth. B 32 (1988) 11.

[7] J.P. Araújo, U.Wahl, E.Alves, J.G.Correia, T.Monteiro, J. Soares, C.Boemare, and the ISOLDE Collaboration, Nucl. Instr. Meth. B 191 (2002) 317.

[8] Commercially available from CrysTec GmbH, 12555 Berlin, Germany

[9] U. Wahl, Hyperfine Interactions 1290 (2000) 349-370

[10] H. Hofsäss and G. Linder, Phys. Rep. 210, (1991) 121

[11] B. C. Chakoumakos, Physica B 241 (1998) 361

[12] N. P. Barradas, M. Rots, A. A. Melo, and J. C. Soares, Phys. Rev. B 47, (1993) 8763